ELSEVIER

Coordination Chemistry Reviews
187 (1999) 103–120

COORDINATION CHEMISTRY REVIEWS

Electronic spectra of cyclotetramolybdenum(II) diynes

William W. Beers [a], Robert E. McCarley [a], Don S. Martin [a], Vincent M. Miskowski [b], Harry B. Gray [b,*], Michael D. Hopkins [c,1]

[a] *Department of Chemistry, Iowa State University, Ames, IA 50011, USA*
[b] *Arthur Amos Noyes Laboratory, California Institute of Technology, Pasadena, CA 91125, USA*
[c] *Department of Chemistry, University of Pittsburgh, Pittsburgh, PA 15260, USA*

Received 5 August 1998; accepted 7 December 1998

Contents

Abstract

Low-temperature electronic-absorption spectra are reported for the tetranuclear Mo(II) clusters $Mo_4Cl_8(PR_3)_4$, R = Et and Bu″ (single crystals and dilute polymer films), and $Mo_4Br_8(PBu^n_3)_4$ (polymer film). The results support a molecular-orbital model in which the δ-bonds of the constituent Mo_2 subunits ($d(Mo_2) = 2.21–2.23$ Å) have been broken in the

* Corresponding author. Tel.: + 1-626-395-6500; fax: + 1-626-449-4159.
E-mail addresses: hgcm@its.caltech.edu (H.B. Gray), mdh1@ums.cis.pitt.edu (M.D. Hopkins)
[1] Also corresponding author. Tel.: + 1-412-624-8420; fax: + 1-412-624-7694.

0010-8545/99/$ - see front matter
PII: S0010-8545(99)00008-9

rectangular clusters with the formation of long-edge Mo–Mo single bonds ($d(Mo_2) \sim 2.9$ Å). There is no significant visible absorption polarized parallel to the short bonds; that is, the prominent metal–metal polarized $^1(\delta \rightarrow \delta^*)$ transition of quadruply bonded $Mo_2X_4(PR_3)_4$ complexes is not observed. A very intense near-UV absorption band at 311 nm (ε 30 600 M^{-1} cm^{-1}) for $Mo_4Cl_8(PBu^n_3)_4$ is assigned to the dipole-allowed $^1(\sigma' \rightarrow \sigma'^*)$ transition associated with the long Mo–Mo bonds. The many weaker absorption systems in the visible spectra, consisting exclusively of bands polarized either parallel to the long Mo–Mo bonds or perpendicular to the Mo_4 plane, are assigned to $\pi \rightarrow \sigma'^*$ transitions and/or forbidden $\sigma' \rightarrow \sigma'^*$ transitions. No electronic emission is observed, nor are transient-absorption signals with lifetimes of greater than 20 ns. Together with the absence of any photochemistry for visible irradiation, the results indicate that the excited states undergo rapid nonradiative decay to the ground state.

Keywords: Electronic spectra; Cyclotetramolybdenum(II) diynes; Dilute polymer films

1. Introduction

Tetranuclear cluster compounds of the type $M_4X_8L_4$ (M = Mo, W; X = Cl, Br, I; L = PR_3, RCN, ROH, tetrahydrofuran) [1] are related to quadruply metal–metal-bonded $M_2X_4L_4$ complexes [2] by a deficiency of L ligands [1]. The crystal structures of the compounds $Mo_4Cl_8(PEt_3)_4$ [1a,3] and $Mo_4Cl_8\{P(OMe)_3\}_4$ [4] reveal a rectangular metal cluster of approximate C_{2h} symmetry. An isomeric rectangular metal cluster structure of D_2 symmetry has been found in a crystal structure determination of the compound $Mo_4Cl_8(PBu^n_3)_4$ [1d,5] as well as for its tungsten and mixed-metal molybdenum–tungsten homologues [1d]. The structures of the two isomers are illustrated below.

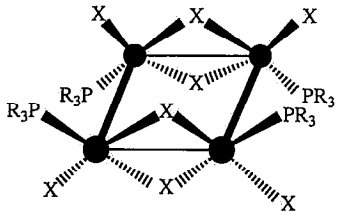

C_{2h}

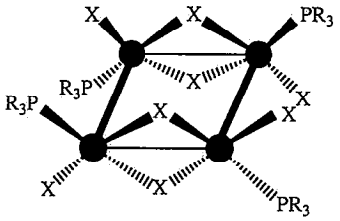

D_2

For both isomeric structures, the unbridged Mo–Mo distances are in the range 2.21–2.23 Å [1,3,4]; this is a typical length for a Mo≡Mo bond [2], and is substantially longer than the quadruple bond length of ca. 2.13 Å for $Mo_2X_4(PR_3)_4$ [2]. The Mo–Mo bonds along the long edges of the Mo_4 rectangle, which are supported by two halide bridges, are ca. 2.9 Å in length, suggestive of metal–metal

single bonds; the dichloride-bridged compounds $Zr_2X_6(PR_3)_4$ [6], which are the closest analogues for the long-edge metal–metal bonding situation that we are aware of, have metal–metal distances of 3.1–3.2 Å and formal metal–metal single bonds [7]. The metal–metal distances of the M_4 units, along with spectroscopic data, led to the proposal [1] that the δ-bond of the parent $M \overset{4}{-} M$ subunits is broken in the M_4 clusters, with the d_{xy} orbitals forming M–M single bonds along the long, doubly bridged edges. This amounts to a formal cycloaddition of two metal–metal quadruply bonded dimers to yield a cyclotetrametalla diyne. A theoretical study [8] of the homoleptic D_{2h} complex $[Mo_4Cl_{12}]^{4-}$ is fully consistent with this description of the bonding.

The electronic-spectroscopic properties of quadruply bonded $M_2X_4(PMe_3)_4$ (M = Mo, W) complexes have been investigated extensively [9]. Aided by these results, and with insights from the theoretical work [8], we have interpreted the electronic spectra of $M_4X_8L_4$ clusters. We also have studied the photophysical and photochemical properties of these clusters.

2. Experimental section

The compounds $Mo_4X_8(PBu^n_3)_4$ (X = Cl, Br) and $Mo_4Cl_8(PEt_3)_4$ were prepared by established methods [1c]. Single crystals of $Mo_4Cl_8(PBu^n_3)_4$ and $Mo_4Cl_8(PEt_3)_4$ were respectively obtained by vapor diffusion of methanol into a concentrated benzene solution and slow evaporation of a solution in 1:1 benzene/hexane. The well developed faces and the crystal directions of their extinctions were identified for crystals mounted on an X-ray diffractometer. Unit-cell dimensions agreed well with reported values [1a,d,3].

Poly(methylmethacrylate) (PMMA) films containing $Mo_4X_8(PR_3)_4$ were cast onto quartz disks from concentrated CH_2Cl_2 solutions by slow evaporation.

Spectrometers, low-temperature equipment, and the Nd:YAG laser system have been described elsewhere [10,11].

3. Results and discussion

3.1. Solution electronic spectra

Electronic-absorption spectra of $Mo_4X_8(PBu^n_3)_4$ (X = Cl, Br) in hexane solution are shown in Fig. 1; the data are summarized in Table 1. Extinction coefficients at the maxima agree within 5–10% with those of a previous report [1a] except for those of the weakest bands ($\lambda > 500$ nm); care has been taken to determine these latter extinction coefficients with better precision in the present work. The UV bands ($\lambda < 300$ nm) have not been previously reported. The spectrum of $Mo_4Cl_8(PEt_3)_4$ in hexane is qualitatively very similar to that of $Mo_4Cl_8(PBu^n_3)_4$ in terms of maxima and relative intensities, but, because of its very low solubility, extinction coefficients were not determined.

Spectra at room temperature and 30 K for PMMA films of $Mo_4Cl_8(PR_3)_4$ (R = Bu^n and Et) are shown in Fig. 2; the data are summarized in Table 2. The room temperature spectra are very similar to those of hexane solutions. Bands at $\lambda > 500$ nm are too weak to yield significant absorption for these thin film samples.

The major bands of these spectra sharpen and significantly blue shift upon cooling. Resolved in each of the spectra are additional features about 30 nm to both higher and lower energy of the intense ca. 310-nm absorption band. The ca. 430-nm band of $Mo_4Cl_8(PEt_3)_4$ develops a high-energy shoulder, but a similar feature is not evident for $Mo_4Cl_8(PBu^n_3)_4$. Spectroscopic data of a PMMA film of $Mo_4Br_8(PBu^n_3)_4$ (spectrum not shown) are included in Table 2. For this compound, no features other than those already evident in the room-temperature spectrum are resolved at 30 K; the temperature dependences of the absorption bands are similar to those exhibited by the bands of the chloro complexes.

3.2. Single-crystal spectra: crystallographic considerations

We show below our definition, to be used throughout the paper, of molecular axes for the tetranuclear compounds. The z-axis was chosen so as to emphasize comparisons to quadruply bonded $Mo_2X_4(PR_3)_4$ compounds [9]; it is also consistent with the axes chosen in a theoretical calculation [8]. The y axis, not indicated in the sketch, is perpendicular to the Mo_4 plane.

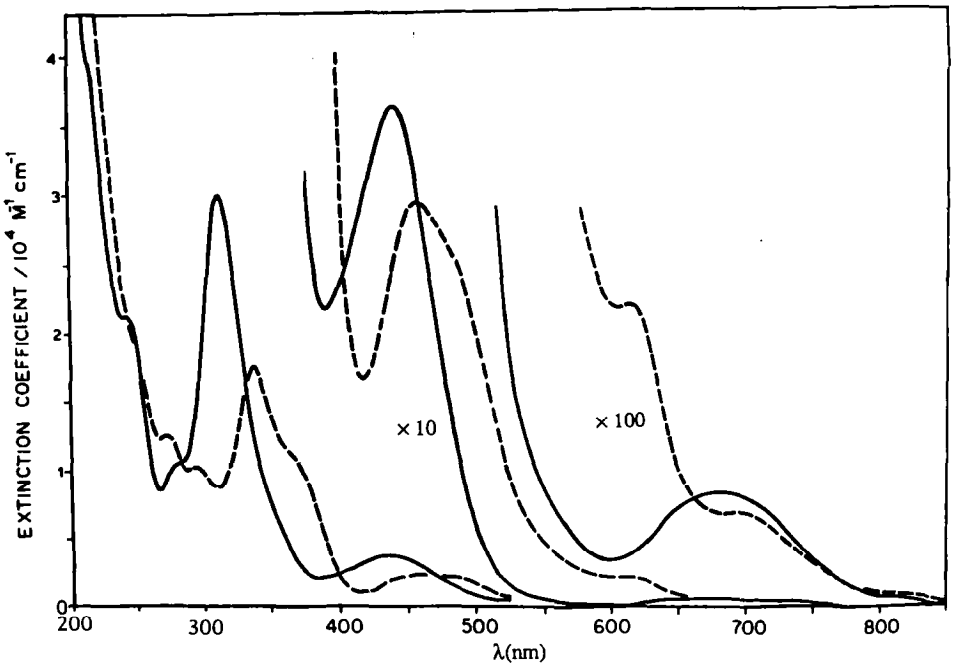

Fig. 1. Electronic spectra of $Mo_4X_8(PBu^n_3)_4$ (hexane solution, room temperature): X = Cl (—); X = Br (---).

Table 1
Absorption spectra of $Mo_4X_8(PBu^n_3)_4$ in hexane solution at room temperature

Compound	λ_{max}/nm	Energy/$cm^{-1} \times 10^3$	$\varepsilon_{max}/M^{-1}\ cm^{-1}$
$Mo_4Cl_8(PBu^n_3)_4$	682	14.7	82
	437	22.9	3700
	311	32.2	30 600
	280	35.7	10 600
	243	41.2	21 700
	215	46.5	40 500 (sh)
$Mo_4Br_8(PBu^n_3)_4$	693	14.4	64
	614	16.3	210
	480	20.8	2600 (sh)
	455	22.0	2900
	367	27.2	12 100 (sh)
	337	29.7	17 000
	295	33.9	11 100
	272	36.8	13 700

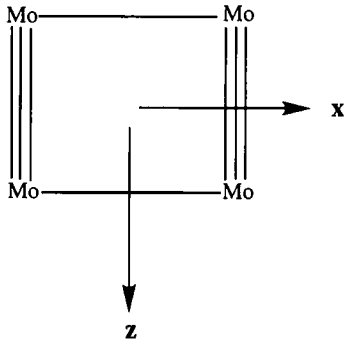

The well developed face of the greenish-yellow crystals of $Mo_4Cl_8(PEt_3)_4$ was identified by X-ray methods as (100) of the monoclinic ($P2_1/c$) lattice. There are two orientations of the molecular unit, owing to a 90° rotational disorder of the Mo_4 unit (exchanging y and z) within the cage of the terminal ligands; the minor orientation occurs, according to Cotton and Shang [3], to the extent of 8%. Beers [12] had earlier refined this disorder in an independent X-ray determination, arriving at a population for the minor orientation of 5%. In Table 3 we present the normalized intensities calculated according to the atomic coordinates of the Cotton and Shang refinement, including an average for the two orientations. Calculation of an average is reasonable because the two crystallographic orientations exhibit no significant internal metric differences; since the observed electronic absorption bands are all broad (widths $\geq 2000\ cm^{-1}$), significant spectral shifts between the two orientations are unlikely. The site symmetry is only $\bar{1}$ but the molecular structure conforms closely to C_{2h} symmetry, and, in particular, the Mo≡Mo and Mo–Mo vectors are precisely orthogonal.

The well developed face of crystals of $Mo_4Cl_8(PBu^n_3)_4$ was identified by X-ray methods as (110) of the orthorhombic space group F_{ddd} [5]. Intensities predicted by electric-dipole selection rules are summarized in Table 4. The site symmetry for this compound conforms to the maximum molecular symmetry, D_2. Rotational Mo_4 disorder of the type found for $Mo_4Cl_8(PEt_3)_4$ was not detected in the crystal-structure refinement [5]. If it occurs to some extent, predictions for x-polarization will be unaffected but the z- and y- polarizations will be mixed into each other.

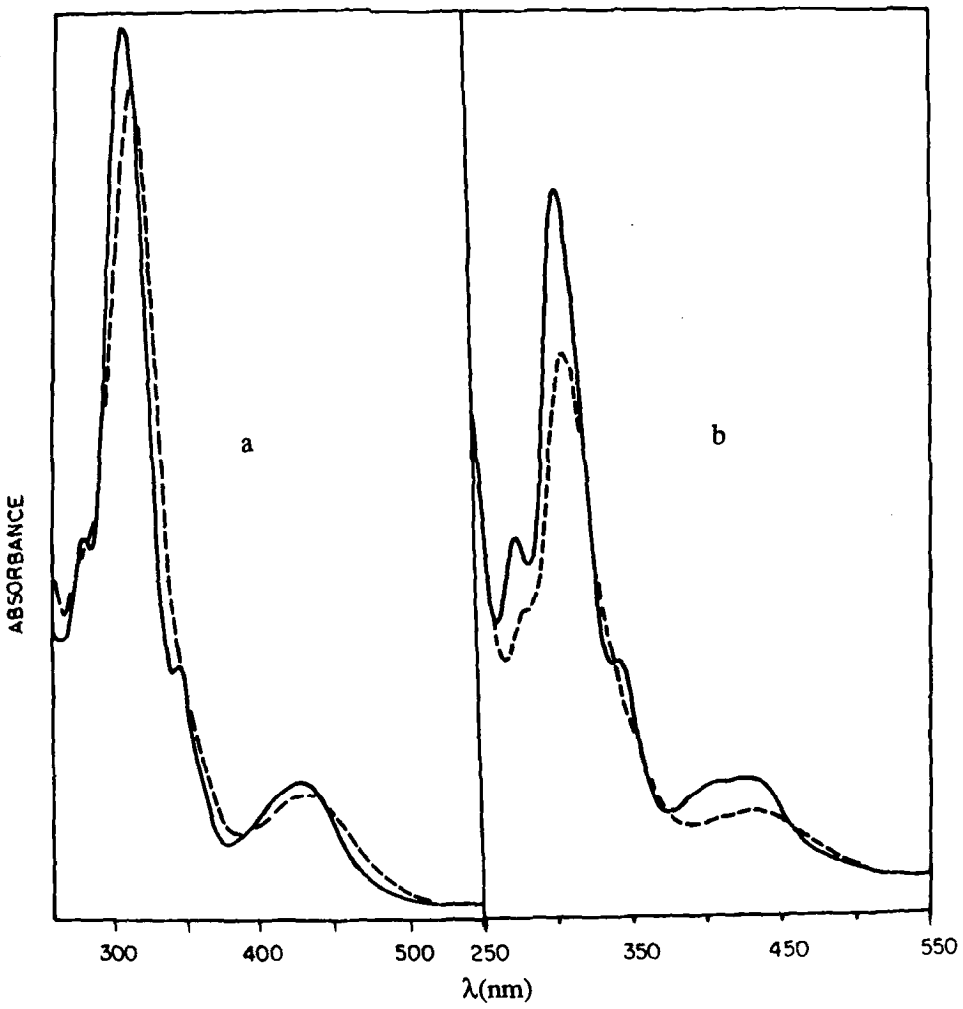

Fig. 2. Electronic spectra of $Mo_4Cl_8(PR_3)_4$ (PMMA film) at 300 K (—) and 30 K (---): (a) R = Bu^n; (b) R = Et.

Table 2
Absorption spectra of $Mo_4X_8(PR_3)_4$ in PMMA films[a]

Compound	$T = 295$ K		$T = 30$ K	
	λ_{max}/nm	Energy/cm$^{-1} \times 10^3$	λ_{max}/nm	Energy/cm$^{-1} \times 10^3$
$Mo_4Cl_8(PBu^n_3)_4$	438	22.8	425	23.5
	[b]	[b]	344	29.1
	310	32.3	302	33.1
	ca. 275 (sh)	ca. 36 (sh)	278	36.0
$Mo_4Cl_8(PEt_3)_4$	431	23.2	427	23.4
	[b]	[b]	ca. 400 (sh)	ca. 25 (sh)
	[b]	[b]	336	29.8
	305	32.8	301	33.2
	ca. 275 (sh)	ca. 36 (sh)	277	36.1
$Mo_4Br_8(PBu^n_3)_4$	470	21.3	471	21.2
	430 (sh)	23 (sh)	432	23.1
	370 (sh)	27 (sh)	363	27.5
	334	29.9	326	30.7
	ca. 300 (sh)	ca. 33 (sh)	291	34.4

[a] Weak bands at $\lambda > 500$ nm were not measured in these experiments.
[b] Not resolved.

3.3. Single-crystal spectra of $Mo_4Cl_8(PBu^n_3)_4$

Fig. 3 shows single-crystal polarized absorption spectra of a thin crystal of $Mo_4Cl_8(PBu^n_3)_4$ at 6 and 300 K and Table 5 summarizes the data. Six distinct absorption features are observed, labeled bands I–VI in Table 5 [13]. The lowest-

Table 3
Calculated relative electric dipole intensities for the (100) crystal face of $Mo_4Cl_8(PEt_3)_4$[a]

Crystal face extinction direction	Molecular transition dipole orientation	Relative intensity		
		Major orientation	Minor orientation	Average over the two orientations[b]
$\|b$	z, $\|$(Mo≡Mo)	0.032	0.995	0.109
	x, $\|$(Mo–Mo)	0.001	0.002	0.001
	y, $\perp(Mo_4)$	0.967	0.001	0.900
$\|c$	z, $\|$(Mo≡Mo)	0.909	0.002	0.836
	x, $\|$(Mo–Mo)	0.068	0.063	0.068
	y, $\perp(Mo_4)$	0.027	0.936	0.100

[a] Molecular transition intensities are defined so as to sum to 1 for the crystal directions $\|b$ and $\|c$ plus a third direction orthogonal to them.
[b] The minor orientation is assumed to be present to the extent of 8%.

Table 4
Calculated relative electric dipole intensities for the (110) crystal face of $Mo_4Cl_8(PBu^n_3)_4$[a,b]

Crystal face extinction direction	Molecular transition dipole orientation	Relative intensity
$\|c$	z, $\|$(Mo≡Mo)	0.999
	x, $\|$(Mo–Mo)	0
	y, $\perp(Mo_4)$	0
$\perp c$	z, $\|$(Mo≡Mo)	0.0005
	x, $\|$(Mo–Mo)	0.651
	y, $\perp(Mo_4)$	0.349

[a] Molecular transition intensities are defined so as to sum to 1 for the two orthogonal directions summarized in the table plus a third direction orthogonal to them.

[b] The Mo_4 unit is very nearly, but not exactly, planar. Calculated intensities for the z and x molecular directions are for the crystallographic Mo≡Mo and Mo–Mo vectors, while that for y is for the vector perpendicular to the average Mo_4 plane.

energy band, I, maximizes at 14 900 cm^{-1} at 6 K and is predominantly polarized $\perp c$. The polarization ratio of band I is not well determined from these data because of baseline problems [14]. Fig. 4 shows the polarized spectra for a thicker crystal at a slightly higher temperature (30 K), where the polarization ratio ($\perp c/\|c$) of this band is better determined.

Reference to Table 4 indicates that band I might be either x- ($\|$(Mo–Mo)) or y- ($\perp Mo_4$) polarized. The small but nonzero $\|c$ intensity of the band is not explained by either assignment (Table 4). The integrated intensity of band I in both polarizations is temperature independent to within 10%; decreases in bandwidth are compensated by increases in peak intensity. However, band I is clearly *not*

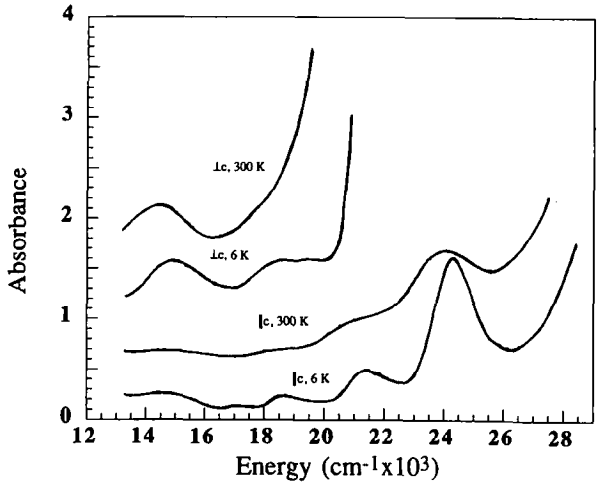

Fig. 3. Polarized electronic spectra for the (110) face of a single crystal of $Mo_4Cl_8(PBu^n_3)_4$ at 6 and 300 K. The various spectra are vertically offset for clarity.

Table 5
Single-crystal absorption spectra of $Mo_4Cl_8(PBu^n_3)_4$

Band	Energy/cm^{-1} × 10^3				Polarization ratio, $\perp c/\|c$		Inferred molecular polarization
	$\perp c$		$\|c$				
	295 K	6 K	295 K	6 K	295 K	6 K	
I	14.4	14.9	14.3	14.8	5.7	4.1	x or y
II	[a]	[a]	[a]	17.0	–	–	?
III	17.6 (sh)	18.5	ca. 18 (sh)	18.3	ca. 6	ca. 4	x or y
IV	[a]	19.6	[a]	[a]	–	–	?
V	[b]	[b]	ca. 21 (sh)	21.4	–	≤5.5[c]	x or y (?)[c]
VI	[b]	[b]	24.0	24.3	–	–	x or y

[a] Not resolved.
[b] Absorption too intense to be recorded.
[c] Polarization ratio at 20 750 cm^{-1}; see text for discussion.

z-polarized; the finite $\|c$ intensity may occur because of some small amount of crystallographically undetected disorder of the type discussed above.

Solution spectra of $Mo_4Cl_8(PBu^n_3)_4$ (Tables 1 and 2) show an intense (ε 3700) band at 22 900 cm^{-1}. The crystal absorption bands in $\|c$ polarization at 24 000 (295 K) and 24 300 cm^{-1} (6 K), band VI, match the solution maximum fairly well, and probably represent a weak $\|c$ component of the intense solution band. This band is thus found to be predominantly $\perp c$ polarized, that is, either x- ($\|$(Mo–Mo)) or y- ($\perp Mo_4$) polarized.

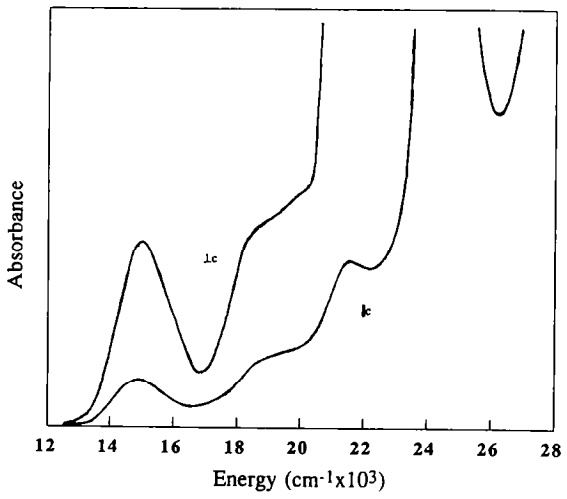

Fig. 4. Polarized electronic spectra for the (110) face of a single crystal of $Mo_4Cl_8(PBu^n_3)_4$ at 30 K. The crystal was thicker than that of Fig. 3.

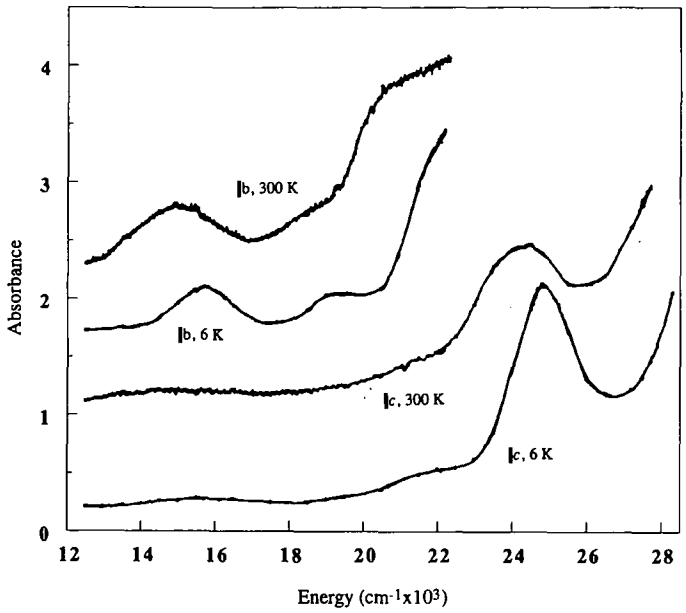

Fig. 5. Polarized electronic spectra for the (100) face of a single crystal of $Mo_4Cl_8(PEt_3)_4$ at 6 and 300 K. The various spectra are vertically offset for clarity.

There are four additional absorption features seen in these spectra (bands II–V, Table 5). None of them are resolved in the solution spectra; hence all four must be extremely weak. Bands II and IV are so weak that neither their polarization nor thermal behavior is established by our data. Band III has a polarization ratio that is similar to that of band I so we again conclude that the band is either x- or y-polarized. The polarization of band V at the maximum is not established because our data in $\perp c$ polarization go offscale a little short of it; the intensity ratio of ca. 5.5 at half-peak-height (20 750 cm^{-1}, the low-energy flank) is a lower limit to the true polarization ratio of this band, and it is similar to those of bands I and III, suggesting x- or y-polarization. However, there is conceivably a substantial contribution to the measured $\perp c$-polarized intensity from more intense, higher-energy bands, so this conclusion is less definitive than for bands I, III, and VI.

3.4. Single-crystal spectra of $Mo_4Cl_8(PEt_3)_4$

Polarized single-crystal spectra of $Mo_4Cl_8(PEt_3)_4$ are shown in Fig. 5; the data are summarized in Table 6. Four bands are observed, which are clearly analogous to bands I, III, V, and VI of $Mo_4Cl_8(PBu^n_3)_4$ and are so labeled in Table 6. Features corresponding to the exceedingly weak bands II and IV of $Mo_4Cl_8(PBu^n_3)_4$ are not resolved.

The orientation of the molecular unit for this crystal face of $Mo_4Cl_8(PEt_3)_4$ is much more suitable for distinguishing between molecular x- and y-polarization

Table 6
Single-crystal absorption spectra of $Mo_4Cl_8(PEt_3)_4$

Band label	Energy/$cm^{-1} \times 10^3$				Polarization ratio, $\|b/\|c$		Inferred molecular polarization
	$\|b$		$\|c$				
	295 K	6 K	295 K	6 K	295 K	6 K	
I	15.0	15.7	ca. 15	ca. 15.5	7	6	*y*
III	18.2 (sh)	19.25	[a]	ca. 19 (sh)	–	ca. 5	*y*
V	20.5 (sh)	21.7 (sh)	ca. 21 (sh)	21.8 (sh)	6[c]	5[c]	*y* (?)[c]
VI	[b]	[b]	24.2	24.9	–	–	*x*[d]

[a] Not resolved.
[b] Absorption too intense to be recorded.
[c] Observed polarization ratio probably affected by overlap with other absorption bands.
[d] See text for discussion.

(Table 3) than is that of the measured crystal face of $Mo_4Cl_8(PBu^n_3)_4$. Thus, whereas data for the latter compound could only be taken to show that band I was either x- or y-polarized, the $Mo_4Cl_8(PEt_3)_4$ data clearly indicate band I to be y-polarized. The experimental polarization ratio, $\|b/\|c \cong 7$, is in good agreement with the theoretical value of 9 from Table 3 for y-polarization (average orientation). The integrated intensity of band I in the $\|b$ polarization decreases by a factor of ca. 2.3 between 295 and 6 K as the band simultaneously sharpens (full-width-at-half-maximum decreases from 2800 to 1800 cm^{-1}) and decreases in peak intensity $(OD)_{max} = 0.525$ and 0.365 for this crystal at 295 and 6 K, respectively). Therefore, the intensity of band I for this compound is largely or entirely vibronically induced. Since the molecular unit of $Mo_4Cl_8(PEt_3)_4$ is located at an inversion center in this crystal [1a,3], we can surmise that band I is Laporte-forbidden; the molecular symmetry of $Mo_4Cl_8(PBu^n_3)_4$ does not include inversion, which accounts for our earlier observation that band I of this compound has temperature-independent intensity.

Bands III and V are weak features that do not contribute appreciably to the solution absorption spectrum. Both of them have polarization similar to band I; their thermal behavior is not well defined because they are shoulders, but predominant y-polarization is evident.

As observed for $Mo_4Cl_8(PBu^n_3)_4$, the maximum of band VI is close to that of a moderately intense solution absorption at 23 000 cm^{-1} and we assume that they correspond. Since our dipole-selection-rule intensity calculations gave good results for band I in this lattice, we can attempt to distinguish between x- and y-polarization for this intense transition (z-polarization being excluded by the feebleness of the $\|c$-polarized intensity) by comparison to the solution spectra, for which band VI is ca. 45 times as intense at the maximum as band I. From Table 3 (final column) we predict that the ratio of the intensities of band VI in $\|c$ polarization and band I (taking band I to be y-polarized) in $\|b$ polarization should be ca. 5 if band VI is y-polarized and ca. 3 if it is x-polarized. The observed value is 2.7, consistent with x-polarization. These calculations definitely show that our correlation of the $\|c$ crystal absorption band VI to the intense solution band is correct; this band must appear in the crystal $\|c$-polarized spectrum with an intensity similar to or greater than the observed intensity of band VI if dipole selection rules are applicable, as they must be for such an intense band.

Assignment of this band to x-polarization is also supported by another aspect of the data. Fig. 3 shows that the $\perp c$-polarized absorption of the $Mo_4Cl_8(PBu^n_3)_4$ crystal goes offscale quite abruptly at 19 400 cm^{-1} (295 K) and 20 800 cm^{-1} (6 K). In contrast, for a crystal of $Mo_4Cl_8(PEt_3)_4$ with a similar absorptivity for band I, the intensely absorbing $\|b$ polarization goes offscale more gently at ca. 22 500 cm^{-1} (Fig. 5). This indicates that intense band VI makes a stronger contribution to the intensely absorbing polarization for the $Mo_4Cl_8(PBu^n_3)_4$ crystal than for the $Mo_4Cl_8(PEt_3)_4$ crystal, which is, according to Tables 3 and 4, consistent with x-polarization, but not with y-polarization. We conclude that band VI is x-polarized.

3.5. Electronic spectral assignments

The electronic spectra of quadruply bonded $Mo_2Cl_4(PR_3)_4$ complexes [9] show three major low-energy bands: ca. 17 000 cm^{-1} (ε 3000 M^{-1} cm^{-1}), $^1(\delta \rightarrow \delta^*)$; ca. 22 000 ($\varepsilon$ 200), $^1(\pi \rightarrow \delta^*)$; ca. 30 000 ($\varepsilon$ 4000), $^1(\sigma(P) \rightarrow \delta^*)$. Note that, unless otherwise specified, the orbitals are metal–metal orbitals. Additional intense LMCT transitions ((Cl, P) $\rightarrow \delta^*$)) are found at considerably higher energy ($\nu > 40\,000$ cm^{-1}) [9c]. The M_2 δ and δ^* levels are depicted in Fig. 6(a).

Upon side-by-side dimerization of M_2 subunits to form a rectangular M_4 cluster, the MO diagrams shown in Figs. 6(b and c) apply [8], where we use symmetry labels appropriate for the parent D_{4h} $[M_2X_8]^{4-}$ and D_{2h} $[M_4X_{12}]^{4-}$ complexes. The two MO diagrams for the M_4 cluster differ depending on whether the magnitude of the metal–metal δ-bond interaction within multiply bonded M_2 subunits is greater than or less than the σ′ dimer–dimer interaction between the d_{xy} orbitals of the two M_2 subunits, the latter being the description favored on structural grounds [1]. Our electronic-spectroscopic results show unequivocally that the structurally based formulation is the correct one.

In the limit $\Delta\delta > \Delta\sigma'$ (Fig. 6(b)), two allowed z-polarized $\delta \rightarrow \delta^*$ transitions, $\delta\sigma'^* \rightarrow \delta^*\sigma'^*$ and $\delta\sigma' \rightarrow \delta^*\sigma'$ are predicted at roughly the same energy as the dimer transition (ca. 17 000 cm^{-1}), flanked by two Laporte-forbidden transitions that are raised or lowered in energy by $\Delta\sigma'$. In the limit $\Delta\sigma' > \Delta\delta$ (Fig. 6(c)), there has been a level crossing, with the result that the two highest-occupied orbitals are now of δ and δ^* parentage. There are two allowed x-polarized $\sigma' \rightarrow \sigma'^*$ transitions, at an energy of $\Delta\sigma'$ in this simple picture, flanked by two Laporte-forbidden transitions

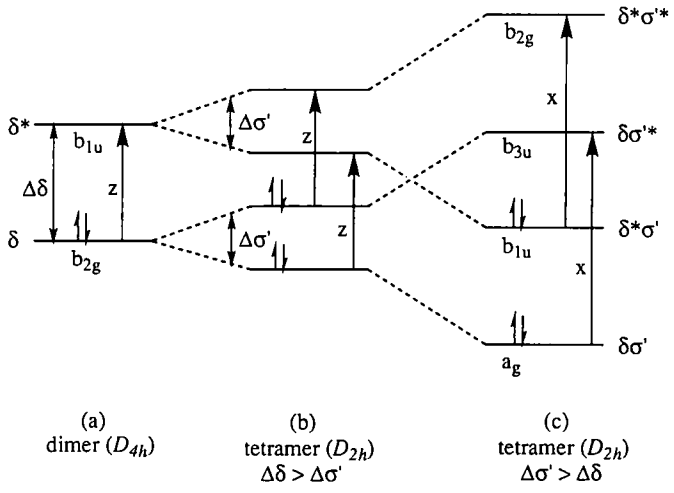

Fig. 6. Molecular-orbital correlation diagram for formation of a rectangular D_{2h} $[M_2]_2$ (= M_4) cluster from two D_{4h} M_2 quadruply bonded binuclear complexes. The prime superscript of σ' distinguishes the interdimer σ-symmetry metal–metal interaction from that (unprimed) of the multiply metal–metal-bonded M_2 subunits. The allowed molecular polarizations are indicated for each transition.

Table 7
Dipole selection rules for the δ/δ^* manifold-derived electronic transitions for the case $\Delta\sigma' > \Delta\delta$ (Fig. 6(c))

Transition	One-electron energy	Allowed polarization		
		D_{2h}	C_{2h}[a]	D_2
$\delta^*\sigma' \rightarrow \delta\sigma'^*$	$\Delta\sigma' - \Delta\delta$	–	–	y
$\delta^*\sigma' \rightarrow \delta^*\sigma'^*$	$\Delta\sigma'$	x	x	x
$\delta\sigma' \rightarrow \delta\sigma'^*$	$\Delta\sigma'$	x	x	x
$\delta\sigma' \rightarrow \delta^*\sigma'^*$	$\Delta\sigma' + \Delta\delta$	–	–	y

[a] Our axis choices make the rotation axis x rather than the conventional z.

that are raised or lowered in energy from $\Delta\sigma'$ by $\Delta\delta$. Since, experimentally, there are no intense z-polarized transitions below ca. 29 000 cm^{-1}, the first model cannot be correct.

Table 7 summarizes dipole-selection rules for the δ/δ^*-derived electronic transitions shown in Fig. 6(c). The two dipole-allowed transitions of the parent D_{2h} symmetry, $\delta^*\sigma' \rightarrow \delta^*\sigma'^*$ and $\delta\sigma' \rightarrow \delta\sigma'^*$, are essentially the $\sigma' \rightarrow \sigma'^*$ transitions of the two long-edge Mo–Mo bonds, and they are x-polarized in our axis system. There is a great deal of information available on $^1(\sigma \rightarrow \sigma^*)$ transitions of singly metal–metal-bonded compounds [15]; for transitions of this type, energies range from 30 000 to 45 000 cm^{-1} and extinction coefficients from 17 000 to 70 000 M^{-1} cm^{-1}. An important characteristic of this type of transition is that there are very drastic thermal effects, the bands broadening and red-shifting with increasing temperature, owing to large excited-state distortions along a low-frequency metal-metal stretching coordinate [15]. In fact, all of the prominent absorption bands of the $Mo_4X_8L_4$ complexes display this type of thermal behavior, which strongly suggests that they involve excitations into σ'^* orbitals; this will result in large distortions along a (presumably low-frequency) $\nu(Mo–Mo)/\delta(Mo_2X_2)$ coordinate. Note that the band maxima and half-widths of the dipole-allowed $^1(\delta \rightarrow \delta^*)$ transitions of $Mo_2Cl_4(PR_3)_4$ exhibit relatively little temperature dependence [9], owing to a relatively small excited-state distortion (ca. 0.1 Å) and a relatively large $\nu(Mo_2)$ frequency (ca. 350 cm^{-1}).

The obvious candidates for the allowed $^1(\sigma' \rightarrow \sigma'^*)$ transitions of $Mo_4X_8(PR_3)_4$ are the intense absorptions seen in isotropic spectra (Figs. 1 and 2) between 300 and 400 nm: 311 nm (ε 30 600 M^{-1} cm^{-1}) for $Mo_4Cl_8(PBu^n_3)_4$; 305 for $Mo_4Cl_8(PEt_3)_4$; 337 (ε 17 000) and 367 (ε 12 100 (sh)) for $Mo_4Br_8(PBu^n_3)_4$. There are no electronic-absorption data available for closely analogous binuclear model complexes such as $Zr_2Cl_6(PR_3)_4$ [2], but the general comparison to binuclear singly bonded compounds [15] is compelling. For example, the $^1(\sigma \rightarrow \sigma^*)$ transition of $[Rh_2(1,3\text{-diisocyanopropane})_4Cl_2]^{2+}$ ($d(Rh_2) = 2.837$ Å) is located at 337 nm (ε 59 000 M^{-1} cm^{-1}) [15a]. Unfortunately, we could not verify whether these bands are x-polarized for the chloro complexes because we could not obtain crystals thin enough to extend the spectra past 355 nm, which is far short of the band maximum.

Other assignments should also be considered for these intense bands. As noted earlier, $Mo_2Cl_4(PR_3)_4$ compounds exhibit a $\sigma(P) \rightarrow \delta^*$ LMCT band near the energy of these bands. However, a similar assignment for $Mo_4X_8(PR_3)_4$ is excluded because: (a) the $Mo_2Cl_4(PR_3)_4$ LMCT band is much weaker ($\varepsilon = 3720$ for $Mo_2Cl_4(PMe_3)_4$) [9a] than the $Mo_4X_8(PR_3)_4$ band; (b) the $Mo_2Cl_4(PR_3)_4$ $\sigma(P) \rightarrow \delta^*$ transition is at particularly low energy among the LMCT transitions [9c] because the relevant e-symmetry $\sigma(P)$ level is nonbonding towards the $d_{x^2-y^2}$ levels [16], whereas all $\sigma(P)$ levels are σ-bonding for C_{2h} or D_2-symmetry $Mo_4X_8(PR_3)_4$ and should therefore be strongly stabilized, raising the energies of the LMCT transitions and (c) most importantly, $Mo_4X_8L_4$ complexes in which the phosphines are replaced by other neutral ligands, such as in $Mo_4Cl_8(EtCN)_4$, display intense absorption bands at very similar energies [1a]. Taken together with the information that other intense LMCT transitions lie at < 250 nm for $Mo_2X_4(PR_3)_4$ compounds [9c], these considerations exclude an LMCT assignment for the 300–400 nm bands of $Mo_4X_8(PR_3)_4$. Intense bands of the tetramers at $\lambda < 300$ nm (Table 1) are attributable to LMCT transitions [9c]. The only other assignment that we consider at all plausible is $^1(\pi \rightarrow \pi^*)$ within the triply bonded Mo_2 units. For quadruply bonded $Mo_2X_4(PMe_3)_4$, this transition has been placed at < 200 nm [9c]; for triply bonded $Mo_2(HPO_4)_4^{2-}$ it has been located at 250 nm [17,18]. It therefore seems unlikely that the intradimer $^1(\pi \rightarrow \pi^*)$ transitions would red-shift to the 300–400 nm region for $Mo_4X_8(PR_3)_4$.

The allowed $^1(\sigma' \rightarrow \sigma'^*)$ assignment thus seems secure for the intense 300–400 nm bands. The compound $Mo_4Br_8(PBu^n_3)_4$ displays a splitting of the band (337 and 367(sh) nm); this conceivably reflects the two nearly degenerate, allowed $^1(\sigma' \rightarrow \sigma'^*)$ transitions that are predicted from Fig. 6 ($\delta\sigma' \rightarrow \delta\sigma'^*$, $\delta^*\sigma' \rightarrow \delta^*\sigma'^*$). The two additional $^1(\sigma' \rightarrow \sigma'^*)$ transitions ($\delta\sigma' \rightarrow \delta^*\sigma'^*$, $\delta^*\sigma' \rightarrow \delta\sigma'^*$) are predicted to be orbitally forbidden in D_{2h} or C_{2h} symmetry (Table 7) and to lie to higher and lower energy of the allowed transitions by the one-electron parameter $\Delta\delta$. For quadruply bonded $Mo_2Cl_4(PR_3)_4$ molecules, $\Delta\delta$ is estimated to be ca. 8000 cm^{-1} [19], so bands II–VI are all at reasonable energies for the lowest-energy $^1(\sigma' \rightarrow \sigma'^*)$ transition, and band I cannot be excluded either, despite its rather large splitting from the allowed $^1(\sigma' \rightarrow \sigma'^*)$ transition of ca. 16 000 cm^{-1}. The energies of these bonding-to-antibonding transitions include large two-electron contributions [15b,19], and one-electron estimates of relative energies may not be valid.

Compounds with metal–metal single bonds typically show '$\pi \rightarrow \sigma^*$' transitions at 5000–10 000 cm^{-1} to lower energy of the $^1(\sigma \rightarrow \sigma^*)$ transition [15]; for example, $Mn_2(CO)_{10}$ has $\sigma \rightarrow \sigma^*$ at 29 740 cm^{-1} (ε 33 700 M^{-1} cm^{-1}) and $\pi \rightarrow \sigma^*$ at 26 700 cm^{-1} (ε 2900 M^{-1} cm^{-1}) [20]. By analogy, $\pi \rightarrow \sigma'^*$ transitions might be expected at 22 000–28 000 cm^{-1} (350–450 nm) for $Mo_4X_8(PR_3)_4$. We also note that the $\pi \rightarrow \delta^*$ transition of $Mo_2Cl_4(PMe_3)_4$ is observed at 22 000 cm^{-1} [9]. These correlations encourage us to assign the crystal band VI (together with its intense solution counterpart at ca. 23 000 cm^{-1}) to a $\pi \rightarrow \sigma'^*$ transition. Dipole-selection rules for $\pi \rightarrow \sigma'^*$ transitions are summarized in Table 8. There are a total of eight one-electron transitions, and the calculation on $[Mo_4Cl_{12}]^{4-}$ [8] shows that the π (binuclear)-derived levels are spread out over ca. 1 eV. We can, therefore, expect several

weak bands in this energy region, thereby explaining the spectral complexity. The $\pi \rightarrow \sigma^*$ transitions of singly metal–metal-bonded compounds are polarized mainly along the metal–metal axis, owing to intensity-stealing from the very intense $^1(\sigma \rightarrow \sigma^*)$ transition [15a,21].

We suggest that band VI is $a_g \rightarrow b_{3u}$ ($\pi_x \rightarrow \delta\sigma'^*$, Table 8), since this transition is dipole-allowed along x and can therefore directly mix with $\sigma' \rightarrow \sigma'^*$ by a nonvibronic mechanism. Detailed assignments of the plethora of remaining weak bands must await higher-level theoretical calculations than the one available [8]. The possible assignments are not limited to those set out in Table 8; for example, band V has an energy and relative intensity consistent [9a] with it being the spin-forbidden (singlet-triplet) counterpart of band VI.

Band I merits special consideration because of its distinctive polarization and thermal behavior. The $\pi \rightarrow \sigma'^*$ transition $a_g \rightarrow b_{2g}$ ($\pi_x \rightarrow \delta^*\sigma'^*$, Table 8) has the correct symmetry properties; it is dipole-forbidden in C_{2h} ($Mo_4Cl_8(PEt_3)_4$, for which it exhibits temperature-dependent intensity), but dipole-allowed in D_2 ($Mo_4Cl_8(PBu^n_3)_4$). However, $a_g \rightarrow b_{2g}$ must lie to higher energy of the assigned $a_g \rightarrow b_{3u}$ transition (at 23 000 cm^{-1}). Moreover, the levels given by the calculation [8] predict that $a_g \rightarrow b_{2g}$ will possess the highest energy among the $\pi \rightarrow \sigma'^*$ transitions. An alternative (and more interesting) assignment is to the forbidden $\sigma' \rightarrow \sigma'^*$ transition $\delta^*\sigma' \rightarrow \delta\sigma'^*$, $b_{1u} \rightarrow b_{3u}$ (Table 7), which also has the correct symmetry properties; the experimental information available cannot distinguish between these two possible assignments.

3.6. Photochemistry and photophysics

Photolysis ($\lambda > 400$ nm) of $Mo_4Cl_8(PBu^n_3)_4$ in hexane or CH_2Cl_2 solution in the absence or presence of potential ligands (CO, PPh_3, CH_3CN [22]) results in no

Table 8
Dipole-selection rules for $\pi \rightarrow \sigma'^*$ transitions[a]

Transition type	Orbital transition (D_{2h})	Allowed polarization		
		D_{2h}	C_{2h}[b]	D_2
$\pi_x \rightarrow \delta\sigma'^*$	$a_g \rightarrow b_{3u}$	x	x	x
	$b_{3u} \rightarrow b_{3u}$	–	–	–
$\pi_y \rightarrow \delta\sigma'^*$	$b_{1g} \rightarrow b_{3u}$	y	y, z	y
	$b_{2u} \rightarrow b_{3u}$	–	–	z
$\pi_x \rightarrow \delta^*\sigma'^*$	$a_g \rightarrow b_{2g}$	–	–	y
	$b_{3u} \rightarrow b_{2g}$	z	y, z	z
$\pi_y \rightarrow \delta^*\sigma'^*$	$b_{1g} \rightarrow b_{2g}$	–	–	x
	$b_{2u} \rightarrow b_{2g}$	–	–	–

[a] The in-plane (π_x) and out-of-plane (π_y) levels are split into gerade and ungerade combinations in D_{2h} and C_{2h} symmetry.

[b] Our axis choices make the rotation axis x rather than the conventional z.

spectral changes. Dichloromethane solutions of $Mo_4Cl_8(PBu^n_3)_4$ are photosensitive to 254-nm irradiation, changing color from yellow to brown, and similar color changes also occur, but much more slowly, upon 313-nm irradiation. The product solutions exhibit a featureless rising absorption that extends across the visible region. This reaction likely involves photo-oxidation of Mo(II) by the halocarbon solvent, similar to a previously documented UV photoreaction of $Mo_2Cl_4(PR_3)_4$ in halocarbon solution [23]. The reaction clearly involves upper excited states (possibly Cl→Mo LMCT states) [9c,23] rather than the low-energy metal–metal excited states.

None of the $Mo_4X_8(PR_3)_4$ clusters exhibit detectable ($\lambda < 850$ nm) luminescence, either as solids or in alkane (hexane or 2-methylpentane) solution, at room temperature or 77 K. We were unable to detect any transient-absorption (or ground-state bleaching) signals with lifetimes greater than 20 ns upon 532 or 355-nm Nd:YAG pulsed-laser excitation of hexane solutions of $Mo_4Cl_8(PBu^n_3)_4$. This result excludes both long-lived excited states and transients that might result from metal–metal or metal–ligand dissociative photochemistry of significant quantum yield.

Evidently, the low-lying excited states of these compounds undergo very rapid nonradiative decay to the ground state. This behavior contrasts strongly to the photophysics of the $Mo_2X_4(PR_3)_4$ compounds, because the binuclear species exhibit intense fluorescence from a long-lived $^1(\delta\delta^*)$ excited state [24,25]. However, since our spectroscopic studies conclusively indicate that the $Mo_4X_8(PR_3)_4$ clusters do not have low-lying excited states of the $\delta\delta^*$ type, this striking difference in behavior is not surprising.

We have assigned the low-energy electronic absorption bands of the tetramers to $\sigma' \rightarrow \sigma'^*$ and $\pi \rightarrow \sigma'^*$ transitions. Electronic emission from triplet excited states of these types is well established [21,26], albeit exclusively in cases where the metal–metal σ-bond is bridged by ligands so that facile metal–metal dissociation [27] is prevented; moreover, none of the published examples shows measureable luminescence in room-temperature fluid solution. Excited-state nonradiative decay is rapid for these molecules, just as it is in the present case. We therefore conclude that low-energy σ*-type excited states of the tetramers are not dissociative because of the bridging ligands, but they are short-lived because very large metal–metal distortions (along the long edges for the tetramers) facilitate nonradiative decay.

Acknowledgements

All good wishes to Professor Ralph G. Pearson on the occasion of his 80th birthday. This work was supported by the National Science Foundation.

References

[1] (a) R.N. McGinnis, T.R. Ryan, R.E. McCarley, J. Am. Chem. Soc. 100 (1978) 7900–7902. (b) R.E. McCarley, T.R. Ryan, C.C. Torardi, in: M.H. Chisholm (Ed.), Reactivity of Metal–Metal Bonds, ACS Symposium Series 155; American Chemical Society; Washington, DC, 1981; pp. 41–60. (c)

T.R. Ryan, R.E. McCarley, Inorg. Chem. 21 (1982) 2072–2079. (d) R.T. Carlin, R.E. McCarley, Inorg. Chem. 28 (1989) 3432–3436.
[2] F.A. Cotton, R.A. Walton, Multiple Bonds Between Metal Atoms, 2nd Edition, Oxford Press, Oxford, 1993.
[3] F.A. Cotton, M. Shang, J. Cluster Sci. 2 (1991) 121–129.
[4] F.A. Cotton, G.L. Powell, Inorg. Chem. 22 (1983) 871–873.
[5] The crystal structure of $Mo_4Cl_8(PBu^n_3)_4$ has not been reported in full detail, although unit cell parameters and important bond lengths have been [1d]; disorder of the *n*-butyl groups of the phosphine ligands resulted in a low-quality structure ($R = 8.9\%$, $R_w = 10.4\%$), with several C–C bond lengths that refined to unreasonable values (range 1.35–1.70 Å) in the disorder model that was adopted; Mo, Cl, and P positions are nonetheless well defined.
[6] F.A. Cotton, M.P. Diebold, P.A. Kibak, Inorg. Chem. 27 (1988) 799–804.
[7] A theoretical calculation on $Zr_2I_6(PH_3)_4$ supports this view of the metal–metal bonding, F.A. Cotton, M. Shang, W.A. Wojtczak, Inorg. Chem. 30 (1991) 3670–3675.
[8] R.A. Wheeler, R. Hoffmann, J. Am. Chem. Soc. 108 (1986) 6605–6610.
[9] (a) M.D. Hopkins, W.P. Schaefer, M.J. Bronikowski, W.H. Woodruff, V.M. Miskowski, R.F. Dallinger, H.B. Gray, J. Am. Chem. Soc. 109 (1987) 408–416. (b) M.D. Hopkins, V.M. Miskowski, H.B. Gray, J. Am. Chem. Soc. 110 (1988) 1787–1793. (c) V.M. Miskowski, H.B. Gray, M.D. Hopkins, Inorg. Chem. 31 (1992) 2085–2091.
[10] P.E. Fanwick, D.S. Martin, T.R. Webb, G.A. Robbins, R.A. Newman, Inorg. Chem. 17 (1978) 2723–2727.
[11] (a) S.F. Rice, H.B. Gray, J. Am. Chem. Soc. 105 (1983) 4571–4575. (b) D.G. Nocera, J.R. Winkler, K.M. Yocom, E. Bordignon, H.B. Gray, J. Am. Chem. Soc. 106 (1984) 5145–5150.
[12] W.W. Beers, Ph. D. Thesis, Iowa State University, 1983.
[13] Scanning to lower energy both for crystals and concentrated solutions did not reveal any absorptions (other than vibrational overtones) of lower energy than the ca. 14,500 cm^{-1} band, for any of the compounds of this study.
[14] The UV-vis detector of the Cary 14 spectrometer (an R955 PMT) becomes increasingly insensitive for $\lambda > 700$ nm. When the spectrometer is operated in the standard fixed-high-voltage mode, this results in the instrumental slit widths becoming larger at longer wavelengths. If the slit widths become comparable to the crystal horizontal width, an artifactually wavelength-dependent baseline absorbance is introduced, since, if the crystal is well masked, a portion of the analyzing beam is deflected by the mask. The data of Fig. 3 clearly suffer from this problem to a small degree, but those of Figs. 4 and 5 do not.
[15] (a) V.M. Miskowski, T.P. Smith, T.M. Loehr, H.B. Gray, J. Am. Chem. Soc. 97 (1975) 7925–7934. (b) V.M. Miskowski, H.B. Gray, in: J. Avery, J.P. Dahl (Eds.), Understanding Molecular Properties, D. Reidel, Dordrecht, 1987; pp. 1–16.
[16] D.R. Root, C.H. Blevins, D.L. Lichtenberger, A.P. Sattelberger, R.A. Walton, J. Am. Chem. Soc. 108 (1986) 953–959.
[17] M.D. Hopkins, V.M. Miskowski, H.B. Gray, J. Am. Chem. Soc. 108 (1986) 959–963.
[18] I.-J. Chang, D.G. Nocera, J. Am. Chem. Soc. 109 (1987) 4901–4907.
[19] M.D. Hopkins, H.B. Gray, V.M. Miskowski, Polyhedron 6 (1987) 705–714.
[20] R.A. Levenson, H.B. Gray, J. Am. Chem. Soc. 97 (1975) 6042–6047.
[21] R.A. Newman, D.S. Martin, R.F. Dallinger, W.H. Woodruff, A.E. Stiegman, C.-M. Che, W.P Schaefer, V.M. Miskowski, H.B. Gray, Inorg. Chem. 30 (1991) 4647–4654.
[22] $Mo_4Cl_8(PBu^n_3)_4$ undergoes a slow (days) thermal reaction with CH_3CN, whose rate is not affected by irradiation. $Mo_4Br_8(PBu^n_3)_4$ is much more thermally reactive with CH_3CN.
[23] W.C. Trogler, H.B. Gray, Nouv. J. Chim. 1 (1977) 475–477.
[24] (a) V.M. Miskowski, R.A. Goldbeck, D.S. Kliger, H.B. Gray, Inorg. Chem. 18 (1979) 86–89. (b) M.D. Hopkins, H.B. Gray, J. Am. Chem. Soc. 106 (1984) 2468–2469. (c) T.C. Zietlow, M.D. Hopkins, H.B. Gray, J. Solid State Chem. 57 (1985) 112–119.
[25] J.R. Winkler, D.G. Nocera, T.L. Netzel, J. Am. Chem. Soc. 108 (1986) 112–119.
[26] (a) A.E. Stiegman, V.M. Miskowski, J. Am. Chem. Soc. 110 (1988) 4053–4054. (b) Y.K. Shin, V.M. Miskowski, D.G. Nocera, Inorg. Chem. 29 (1990) 2308–2313. (c) J.I. Dulebohn, D.L. Ward, D.G. Nocera, J. Am. Chem. Soc. 112 (1990) 2969–2977. (d) S.J. Milder, M.P. Castellane, T.J.R. Weakly, D.R. Tyler, V.M. Miskowski, A.E. Stiegman, J. Phys. Chem. 94 (1990) 6599–6603.
[27] T.J. Meyer, J.V. Caspar, Chem. Rev. 85 (1985) 187–218.